Biosensors and Bioelectronics 24 (2009) 1141–1145

Contents lists available at ScienceDirect

Biosensors and Bioelectronics

journal homepage: www.elsevier.com/locate/bios

A novel hydrogen peroxide sensor based on the direct electron transfer of horseradish peroxidase immobilized on silica–hydroxyapatite hybrid film

Bin Wang[a], Jing-Jing Zhang[a], Zhuang-Ying Pan[a], Xu-Quan Tao[b], Huai-Sheng Wang[a,b,*]

[a] College of Chemistry and Chemical Engineering, Liaocheng University, Liaocheng 252059, China
[b] College of Materials Science and Engineering, Liaocheng University, Liaocheng 252059, China

ARTICLE INFO

Article history:
Received 12 April 2008
Received in revised form 22 June 2008
Accepted 25 June 2008
Available online 10 July 2008

Keywords:
Hydroxyapatite
Horseradish peroxidase
Biosensor
Hydrogen peroxide
Silica

ABSTRACT

The direct electron transfer of immobilized horseradish peroxidase (HRP) on silica–hydroxyapatite (HAp) hybrid film-modified glassy carbon electrode (GCE) and its application as H_2O_2 biosensors were investigated. On silica/HRP–HAp/GCE, HRP displayed a fast electron transfer process accompanied with one proton participate in. This sensor exhibited an excellent electrocatalytic response to the reduction of H_2O_2 without the aid of an electron mediator. The proposed biosensor showed good reproducibility and high sensitivity to H_2O_2 with the detection limit of 0.35 μM. In the range of 1.0–100 μM, the catalytic reduction current of H_2O_2 was proportional to H_2O_2 concentration. The apparent Michaelis–Menten constant (k_m^{app}) of the biosensor was calculated to be 21.8 μM, exhibiting a high enzymatic activity and affinity for H_2O_2.

1. Introduction

The determination of hydrogen peroxide is of great importance in pharmaceutical, clinical, industrial, and environmental analyses. Many techniques have been employed for the determination of H_2O_2, such as, titrimetry (Hurdis and Romeyn, 1954), spectrometry (Matsubara et al., 1992), chemiluminescence (Nakashima et al., 1991) and electrochemistry (Chen et al., 2007). Among these techniques, the electrochemical method displays better prospect due to its advantages of easy preparation, fast detection, low consume and high sensitivity (Xiao et al., 1999). Many heme proteins show better catalysis to the reduction of H_2O_2 due to the interior electroactive iron hemes. Horseradish peroxidase (HRP), a heme enzyme, is generally used as a representative to investigate the dynamic and thermodynamic mechanism of the enzyme reactions and develop biosensors for the determination of H_2O_2 or related compounds. However, at the bare electrode, HRP does not display electroactivity due to the deep burying of the electroactive groups within the protein structure, unfavorable orientation (Zhang et al., 2007). In order to prepare excellent biosensors, many materials were employed to improve the microenvironment around proteins, provide suitable orientation, and accelerate the electron transfer between protein and the electrode surface. For example, when electrodes were modified with nanoparticles (Zhang et al., 2007; Liu and Ju, 2002; Liu et al., 2008), conducting polymers (Xua et al., 2007; Kong et al., 2003; Huang and Hu, 2003), biomolecules films (Song et al., 2006; Tang et al., 2003; Xiao et al., 2000), redox dye (Salomi and Mitra, 2007), and ionic liquid (Yan et al., 2007), HRP showed direct electrochemical behavior and good electrocatalytic ability to the reduction of H_2O_2. However, the lifetime and the sensitivity of the H_2O_2 biosensors are not satisfied for the determination of H_2O_2 in practical sample.

Hydroxyapatite [HAp, $Ca_{10}(PO_4)_6(OH)_2$] is predominant inorganic component of human bones and teeth, and it has been widely used as bone implant materials or a carrier for genes and enzyme (Barroug and Glimcher, 2002; Matsuda et al., 2003; Wolff and Lederberg, 1994). Some studies have demonstrated that HAp can be used for the preparation of sensors, such as CO gas sensor (Mahabole et al., 2005), CO_2 gas sensor (Nagai et al., 1988, 1990) and phosphate sensor (Petrucelli et al., 1996), due to its porous structure. HAp has been employed also as a support for the chromatographic separation of biological macromolecules (Niu et al., 2006; Useh et al., 2006). In our previous work, we have studied the interaction of DNA with redox-active molecules and the detection of DNA damage with HAp–DNA-modified electrodes (Wang et al., 2005a,b). In these studies, HAp exhibits excellent biocompatibility and adsorbility for the immobilization of DNA.

* Corresponding author at: College of Chemistry and Chemical Engineering, Liaocheng University, Liaocheng 252059, China. Tel.: +86 635 8239860; fax: +86 635 8239860.
E-mail addresses: hswang@lcu.edu.cn, huaishengwang@yahoo.com.cn (H.-S. Wang).

0956-5663/$ – see front matter © 2008 Elsevier B.V. All rights reserved.
doi:10.1016/j.bios.2008.06.053

Many studies have demonstrated the multiple interaction between HAp and proteins, such as the electrostatic attractive force between the carboxylate group and Ca cations on the HAp surface, the intermolecular H-bonds between the *N*-containing group and the phosphate on the HAp surface, and the cooperativity of multiple functional groups of proteins and Ca cations and phosphates on the HAp surface (Jennissen, 1981; Zhou et al., 2007). The adsorption of human serum albumin at HAp-modified silver electrodes by piezoelectric quartz crystal impedance analysis and the fabrication of a label-free capacitive immunosensor based on the immobilization of antibody on HAp for the detection of transferrin were reported by the same research group (Tian et al., 2004; Yang et al., 2005). So, proteins should be adsorbed on HAp firmly and retained its activity.

Silica-based materials are robust inorganic solids, which have high specific surface area and also a three-dimensional structure with highly open spaces interconnected to each other. This material has also the property that can be used as efficient support for enzymes without preventing its biological activity (Lev et al., 1995; Kulys, 1999; Walcarius, 2001).

In this paper, a novel H_2O_2 sensor (silica/HRP–HAp/GCE) was constructed with HAp nanoparticles used as a matrix for HRP immobilization and the silica acted as a fixed reagent to enhance the stability of the sensor. The resulted sensor exhibits excellent electrocatalytic response to the reduction of H_2O_2, better stability and sensitivity than that prepared with the silica only.

2. Experimental

2.1. Reagents and materials

HRP was purchased from Sigma and used without further purification. Tetraethoxysilane (TEOS, 99%) was purchased from Alfa Aesar, H_2O_2 (30%) was purchased from Nanjing Sunshine Biotechnology Ltd., China. All other reagents were of analytical grade. The stock solutions were stored at a temperature of 4 °C. All aqueous solutions were prepared with doubly distilled water.

Electrochemical experiments were carried out on CHI-660B electrochemical working station (CH Instruments Inc., USA), with modified glassy carbon electrode (GCE, CH Instruments Inc., USA, 0.07065 cm^2) as working electrode, platinum wire as counter electrode and saturated calomel reference electrode (SCE). The pH values were determined with a pHs-3C pH meter (Shanghai Analytical Instrument Factory, China). All measurements were carried out at laboratory temperature (about 25 °C), and experimental solutions were deoxygenated by bubbling highly pure nitrogen for 5 min, then a nitrogen atmosphere was kept over the solutions during measurements.

UV–vis absorbance spectroscopy was performed using a HP-8453 UV–vis spectrophotometer (USA). The HRP–HAp (0.08 and 1 mg mL^{-1}) mixture for spectroscopic analysis was confected by mixing appropriate HRP and HAp nanoparticles sol in 0.1 M pH 7.0 PBS and placed for 2 h. The UV–vis spectra were recorded by subtracting the background of 1 mg mL^{-1} HAp nanoparticles sol. All the measurements were carried out at room temperature.

2.2. Preparation of nano-HAp sol, silica sol and silica/HRP–HAp/GCE

The preparation of HAp nanoparticles sol had been described in our previous work (Wang et al., 2005b). Briefly, 0.010 M phosphoric acid solution was dripped to a stirred saturated calcium hydroxide solution at a rate of about 5 mL min^{-1}, until the pH value of the solution reached 8.2. Then the mixture was placed for 12 h, filtrated and rinsed with doubly distilled water and ethanol for two times, respectively. Thereafter, the HAp nanoparticles were dispersed into doubly distilled water by sonicating for about 20 min until a homogeneous sol was obtained.

Silica sol was prepared according to the literature (Wang et al., 2004): 600 μL ethanol, 50 μL TEOS, 10 μL 5 mM NaOH and 60 μL H_2O were mixed thoroughly in a small test tube, sonicating for several minutes. Then the silica sol was obtained.

The HRP–HAp (2.0 and 10 mg mL^{-1}) stock solution for modifying electrode is prepared by adding appropriate HRP into HAp nanoparticles sol.

GCE was polished on chamois leather with alumina slurry, washed in an ultrasonic bath for a few minutes and dried in air before it was modified. Then 8 μL HRP–HAp stock solution was dripped and spread out evenly on the freshly pretreated GCE surface and dried in air. Thereafter, 10 μL silica sol was dripped on the electrode and dried in air. Subsequently, the silica/HRP–HAp/GCE was formed. The modified electrode was washed with doubly distilled water prior to experiment and stored in pH 7.0 PBS at 4 °C when it was not in use.

As a comparison, silica/HAp/GCE and silica/HRP/GCE were prepared in the similar method.

3. Results and discussion

3.1. Spectroscopic analysis of the interaction between HRP and HAp

UV–vis absorbance spectroscopy is usually employed to characterize the conformational change of protein and the interaction between protein and other composition (Zhu et al., 2002). As shown in Fig. 1, the Soret band of HRP presents at 403 nm in 0.1 M pH 7.0 PBS. In the presence of HAp nanoparticles, the absorption band at 403 nm has no shift except the erect movement of the whole curve which indicated that the interaction between the HRP and HAp did not destroy the natural structure or change the fundamental microenvironment of HRP. So the HAp should be an ideal matrix for immobilizing proteins and retaining its activity.

3.2. The direct electrochemical behavior of HRP at silica/HRP–HAp/GCE

The electrochemical behavior of different modified electrodes in 0.1 M pH 7.0 PBS was studied using cyclic voltammetry and the results were shown in Fig. 2A. It can be seen that no electrochemical signals presented at silica/HAp/GCE due to the

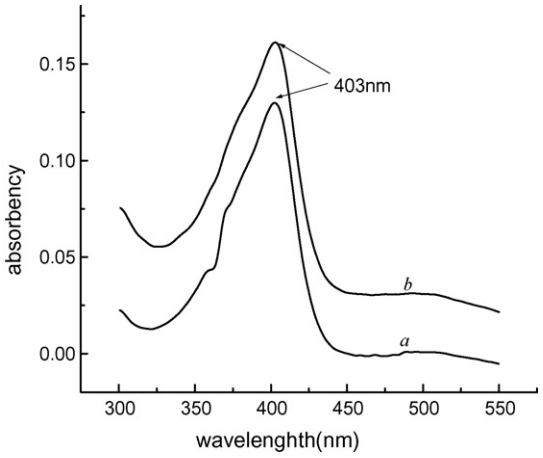

Fig. 1. UV–vis absorption spectra of 0.08 mg mL^{-1} HRP in the absence (*a*) and presence of 1 mg mL^{-1} HAp nanoparticles sol (*b*) in 0.1 M pH 7.0 PBS (curve *b* was recorded by subtracting the background of 1 mg mL^{-1} HAp nanoparticles sol).

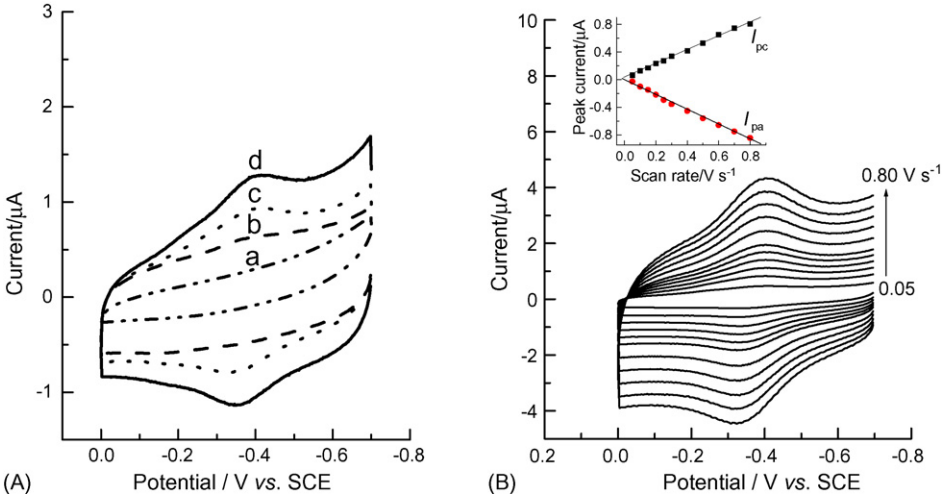

Fig. 2. The cyclic voltammograms of silica/HAp/GCE (a), HRP/HAp/GCE (b), silica/HRP/GCE (c) and silica/HRP–HAp/GCE (d) in 0.1 M pH 7.0 PBS at 0.10 V s^{-1} (A) and the cyclic voltammograms of silica/HRP–HAp/GCE in 0.1 M pH 7.0 PBS at different rates (B). Inset plot in B: the relationship of peak currents versus scan rates.

electro-inactivity of HAp and silica sol in the potential window. At HRP/HAp/GCE, a couple of broad redox peak of HRP appeared with large peak-to-peak potential separation. While at silica/HRP/GCE and silica/HRP–HAp/GCE, the HRP exhibited well-defined redox peaks in the same conditions. At silica/HRP/GCE, the formal potential ($E^{o\prime}$) of HRP was −0.35 V at a scan rate of 0.10 V s^{-1}, which was in accordance with the characteristic potential of the heme Fe(III)/Fe(II) couple in HRP (Zhang et al., 2004). The peak-to-peak potential separation (ΔE) of the redox peaks was about 0.075 V. At silica/HRP–HAp/GCE, the formal potential and peak potential separation values were −0.37 and 0.065 V, respectively. The experiment results demonstrate that the hybrid matrix of silica–HAp can provide a biocompatible microenvironment for HRP and supply a necessary pathway for its direct electron transfer. Thus, HRP gives good electrochemical response at the silica/HRP–HAp/GCE due to the cooperative effect of HAp nanoparticles with silica.

Fig. 2B shows the cyclic voltammograms of HRP at silica/HRP–HAp/GCE in 0.1 M pH 7.0 PBS at different scan rates. In the range of 0.05–0.80 V s^{-1}, both the anodic and cathodic peak current of HRP are directly proportional to the scan rates (inset plot in Fig. 2B), which suggesting a typical surface-controlled electrochemical process. The anodic and cathodic peak potentials did not change apparently with the increasing of scan rate maybe due to the fast electron transfer process between HRP and the electrode surface. The above results also demonstrated that the hybrid film might provide HRP with a favorable microenvironment for facilitating electron transfer. The average surface coverage of HRP was calculated to be 2.13×10^{-11} mol cm^{-2}, according to the peak area of HRP in the cyclic voltammogram.

3.3. The effect of pH on the electrochemical properties of HRP

Fig. 3 shows the effect of pH on electrochemical behavior of HRP. It can be seen from Fig. 3 that the redox peaks of HRP at the silica/HRP–HAp/GCE shift negatively with the increase of pH. In the pH range of 3.0–9.0, the redox peak currents increase and the peak potential separation (ΔE) decrease accordingly with the increase of pH. Such as, the ΔE of HRP is 0.105 and 0.063 V at pH 3.0 and 9.0, respectively. These results suggest that high pH is favorable to the electron transfer between HRP and the electrode surface in the hybrid film. The slop of the formal potential ($E^{o\prime}$) versus pH is estimated to be −0.047 V pH^{-1}, indicating that one proton participates in the electrochemical reaction process (Sun et al., 2000).

3.4. The electrocatalytic properties of silica/HRP/GCE and silica/HRP–HAp/GCE toward the reduction of H_2O_2

The electrocatalytic properties of the two modified electrodes toward the reduction of H_2O_2 were investigated using cyclic voltammetry. As shown in Fig. 4, both the silica/HRP/GCE and silica/HRP–HAp/GCE give a couple of redox peak of HRP in 0.1 M pH 7.0 PBS (curves *a* and *b*), respectively. In the presence of 40 μM H_2O_2, the cathodic peak currents of HRP at the silica/HRP/GCE and silica/HRP–HAp/GCE were increased and the anodic peak currents were disappeared completely (curves *a′* and *b′*). The phenomena indicated the evident catalytic effect of HRP to the reduction of H_2O_2. The electrocatalytic process could be expressed as the follows:

$$\text{Heme–Fe}^{2+} + H_2O_2 \rightarrow \text{Heme–Fe}^{3+} + H_2O$$

$$\text{Heme–Fe}^{3+} + e^- \rightarrow \text{Heme–Fe}^{2+}$$

It can be seen also from Fig. 4 that the catalytic reduction current of H_2O_2 at the silica/HRP–HAp/GCE (curve *b′*) is higher than that at the silica/HRP/GCE (curve *a′*) in the presence of 40 μM H_2O_2. This result suggests that the silica/HRP–HAp/GCE, as a sensor, has

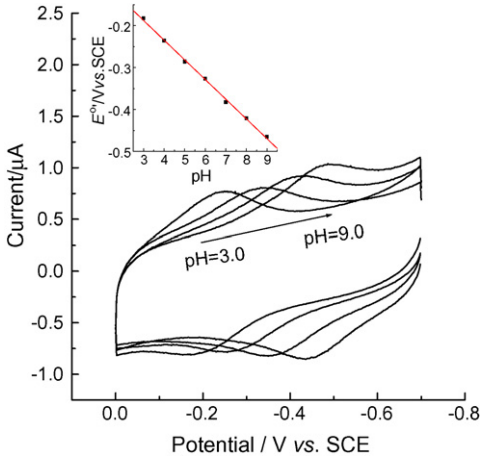

Fig. 3. The cyclic voltammograms of silica/HRP–HAp/GCE in 0.1 M PBS at different pH at scan rate of 0.10 V s^{-1}. Inset plot: the relationship of formal potential versus pH.

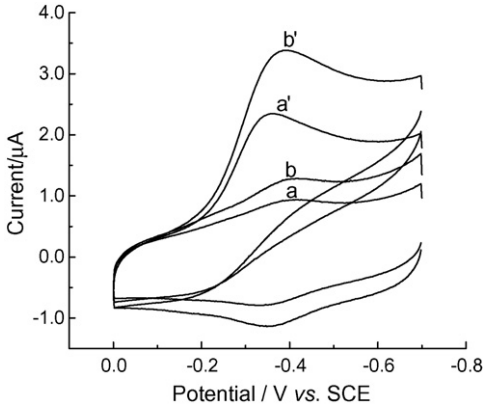

Fig. 4. Cyclic voltammograms of silica/HRP/GCE (*a* and *a*′) and silica/HRP–HAp/GCE (*b* and *b*′) in the absence (*a* and *b*) and presence (*a*′ and *b*′) of 40 μM H_2O_2 in 0.1 M pH 7.0 PBS. Scan rate is 0.10 V s^{-1}.

a higher sensitivity for the detection of H_2O_2 than silica/HRP/GCE has. The reason for it may be that more HRP are immobilized on silica–HAp composite film due to the interaction between HRP and HAp and the presence of the outer silicate film which can protect the HRP layer from the external solution and prevent HRP leaching. The results also suggest that the microporous structure of the silica–HAp composite film not only provide a biocompatible microenvironment for HRP immobilization, but also a necessary pathway for its electron transfer and H_2O_2 diffusion.

In order to optimize the experimental condition, the effect of the pH on the electrochemical response of the biosensor in the presence of 40 μM H_2O_2 was studied using the cyclic voltammetry. The results demonstrate that the reduction peak current of the biosensor attained the maximum value at pH 7.0. Thus, 0.1 M pH 7.0 PBS was selected as the supporting electrolyte for the determination of H_2O_2. The applied potential of the sensor was investigated by chronoamperometry, and −0.40 V was selected as working potential.

In order to compare the electrochemical responses of silica/HRP/GCE and silica/HRP–HAp/GCE to the reduction of H_2O_2, the current–time responses for the continuous addition of H_2O_2 were recorded and the results were shown in Figs. 5 and 6. For silica/HRP/GCE (Fig. 5), it can be seen that the catalytic reduction current of H_2O_2 was directly proportional to the H_2O_2 concentration in the range of 4.0–44 μM although the response current was not steady enough. The detection limit was estimated to be 1.0 μM ($S/N = 3$), and the sensitivity was calculated to be 30.7 mA M^{-1}. The steady state current achieved 95% of the maximum at about 10 s. As for silica/HRP–HAp/GCE (Fig. 6), the steady state current was linear with the H_2O_2 concentration in the range of 1.0–100 μM. The linear regression equation was $I/\mu A = 0.2770 + 0.0506c/\mu M$, with a correlation coefficient of 0.9990 ($n = 21$). From the slope of the regression equation, the detection limit and sensitivity of the biosensor was estimated to be 0.35 μM ($S/N = 3$) and 50.56 mA M^{-1}, respectively. In comparison with other methods (Yang et al., 2008; Zhao et al., 2008), the detection limit was lower and the sensitivity was higher. The steady state current achieved 95% of the maximum at about 5 s. The above results demonstrate that HRP immobilized on HAp–silica hybrid film exhibited higher catalytic ability and fast response for H_2O_2 reduction than immobilized on silica film. Thus, silica/HRP–HAp/GCE as the biosensor has high sensitivity for the detection of H_2O_2.

At silica/HRP–HAp/GCE, when the H_2O_2 concentration was more than 0.12 mM, a response platform was observed, showing the characteristics of Michaelis–Menten kinetics. The apparent Michaelis–Menten constant (k_m^{app}) could be calculated from the Lineweaver–Burk equation: $1/I_{ss} = 1/I_{max} + k_m^{app}/I_{max}c$ (Kamin and Wilson, 1980).

Here I_{ss}, I_{max} and c represent the steady current, maximum current and H_2O_2 concentration, respectively. It is well known that a smaller k_m^{app} implies a higher catalytic activity of the immobilized enzyme.

Based on the Lineweaver–Burk equation, the k_m^{app} of silica/HRP/GCE and silica/HRP–HAp/GCE were calculated to be 53.2 and 21.8 μM, respectively. The results demonstrate that the interaction between HAp and HRP could improve the properties of the biosensor and enhanced the affinity of HRP to H_2O_2.

3.5. Reproducibility and stability of the biosensor

The silica/HRP–HAp/GCE show good stability in 0.1 M pH 7.0 PBS upon continuous cyclic voltammetric sweep over the potential range of −0.7 to 0 V. After continuous sweep for 2 h, the peak current decreased only 4.1%. After the modified electrode was stored in 0.1 M pH 7.0 PBS at 4 °C for 2 weeks, the peak current of the modified electrode retained 95% of its initial value. To investigate the

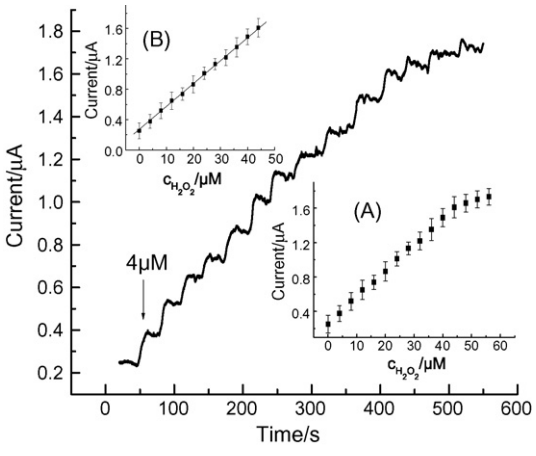

Fig. 5. Typical steady-state current–time response of silica/HRP/GCE with successive additions of 4.0 μM H_2O_2 to the 0.1 M pH 7.0 PBS. Applied potential was −0.40 V (inset A: the relationship of catalytic current with the concentration of H_2O_2; inset B: the calibration curve of the biosensor).

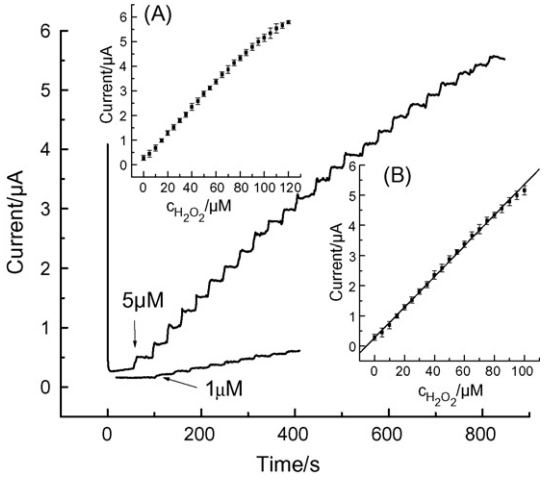

Fig. 6. Typical steady-state current-time response of silica/HRP–HAp/GCE upon successive additions of 1 μM and 5 μM H_2O_2 to the 0.1 M pH 7.0 PBS. Applied potential was −0.40 V (inset A: the relationship of catalytic current with the concentration of H_2O_2; inset B: the calibration curve of the biosensor).

reproducibility of the sensor, six sensors were fabricated in similar method. The relative standard deviation for the determination of 50 μM H_2O_2 was 5.2% for the six sensors.

4. Conclusions

HRP is successfully immobilized on GCE with HAp and silica nanoparticles hybrid film. As a bioinorganic material, HAp shows excellent biocompatibility and affinity for the immobilization of HRP. The resulting modified electrode, silica/HRP–HAp/GCE, can be used as a biosensor for the detection of H_2O_2, which shows wider linear detection range, lower detection limit, and higher sensitivity than the pure silica nanoparticles modified electrode has. The results demonstrate that HAp nanoparticles can provide good microenvironment for the immobilization of protein. This study can provide a new strategy for further study on the direct electron transfer of proteins and the development of biosensors.

Acknowledgements

Financial supports from the National Natural Science Foundation of China (nos. 20475024 and 20775031) and Shandong Tai-Shan Scholar Research Fund are gratefully acknowledged.

References

Barroug, A., Glimcher, M.J., 2002. J. Orthop. Res. 20, 274–280.
Chen, H.J., Wang, Y.L., Liu, Y., Wang, Y.Z., Qi, L., Dong, S.J., 2007. Electrochem. Commun. 9, 469–474.
Huang, R., Hu, N.F., 2003. Biophys. Chem. 104, 199–208.
Hurdis, E.C., Romeyn Jr., H., 1954. Anal. Chem. 26 (2), 320–325.
Jennissen, H.P., 1981. Adv. Enzyme Regul. 19, 377–406.
Kamin, R.A., Wilson, G.S., 1980. Anal. Chem. 52, 1198–1205.
Kong, Y.T., Boopathi, M., Shim, Y.B., 2003. Biosens. Bioelectron. 19, 227–232.
Kulys, J., 1999. Biosens. Bioelectron. 14, 473–479.
Lev, O., Tionsky, M., Rabinovich, L., Glezer, V., Sampath, S., Pankratov, I., Gun, J., 1995. Anal. Chem. 67, 22A–30A.
Liu, S.Q., Ju, H.X., 2002. Anal. Biochem. 307, 110–116.
Liu, Y., Lei, J.P., Ju, H.X., 2008. Talanta 74 (4), 965–970.
Mahabole, M.P., Aiyer, R.C., Ramakrishna, C.V., Sreedhar, B., Khairnar, R.S., 2005. Bull. Mater. Sci. 28 (6), 535–545.
Matsubara, C., Kawamoto, N., Takamura, K., 1992. Analyst 117, 1781–1784.
Matsuda, A., Furuzono, T., Walsh, D., Kishida, A., Tanaka, J., 2003. J. Mater. Sci. Mater. Med. 14, 973–978.
Nagai, M., Nishino, T., Saeki, T., 1988. Sensors Actuat. B 15, 145–151.
Nagai, M., Saeki, T., Nishino, T., 1990. J. Am. Ceram. Soc. 73 (5), 1456–1460.
Nakashima, K., Maki, K., Kawaguchi, S., Akiyama, S., Tsukamoto, Y., Kazuhiro, I., 1991. Anal. Sci. 7, 709–714.
Niu, J.F., Wang, G.C., Tseng, C.K., 2006. Protein Exp. Purif. 49 (1), 23–31.
Petrucelli, G.C., Kawachi, E.Y., Kubota, L.T., Bertran, C.A., 1996. Anal. Commun. 33, 227–229.
Salomi, B.S.B., Mitra, C.K., 2007. Biosens. Bioelectron. 22, 1825–1829.
Song, Y.H., Wang, L., Ren, C.B., Zhu, G.Y., Li, Z., 2006. Sensors Actuat. B 114, 1001–1006.
Sun, H., Hu, N.F., Ma, H.Y., 2000. Electroanalysis 12, 1064–1070.
Tang, J.L., Wang, B.Q., Wu, Z.Y., Han, X.J., Dong, S.J., Wang, E.K., 2003. Biosens. Bioelectron. 18, 867–872.
Tian, L., Wei, W.Z., Mao, Y.A., 2004. Anal. Sci. 20, 623–626.
Useh, N.M., Ajanusi, J.O., Esievo, K.A.N., Nok, A.J., 2006. Cell Biochem. Funct. 24 (4), 347–352.
Walcarius, A., 2001. Electroanalysis 13, 701–718.
Wang, G.X., Pan, Q.X., Wang, H.S., 2005a. Chem. J. Chin. Univ. 26, 1812–1816.
Wang, H.S., Wang, G.X., Pan, Q.X., 2005b. Electroanalysis 17, 1854–1860.
Wang, Q.L., Lu, G.X., Yang, B.J., 2004. Biosens. Bioelectron. 19, 1269–1275.
Wolff, J.A., Lederberg, J., 1994. Human Gene Ther. 5, 469–480.
Xiao, Y., Ju, H.X., Chen, H.Y., 1999. Anal. Chim. Acta 391, 73–82.
Xiao, Y., Ju, H.X., Chen, H.Y., 2000. Anal. Biochem. 278, 22–28.
Xua, Q., Zhua, J.J., Hu, X.Y., 2007. Anal. Chim. Acta 597, 151–156.
Yan, R., Zhao, F.Q., Li, J.W., Xiao, F., Fan, S.S., Zeng, B.Z., 2007. Electrochim. Acta 52, 7425–7431.
Yang, L., Wei, W.Z., Gao, X.H., Xia, J.J., Tao, H., 2005. Talanta 68, 40–46.
Yang, X.S., Chen, X., Zhang, X., Yang, W.S., Evans, D.G., 2008. Sensors Actuat. B 129, 784–789.
Zhang, L., Zhang, Q., Lu, X.B., Li, J.H., 2007. Biosens. Bioelectron. 23, 102–106.
Zhang, Y., He, P.L., Hu, N.F., 2004. Electrochim. Acta 49, 1981–1988.
Zhao, X.J., Mai, Z.B., Kang, X.H., Zou, X.Y., 2008. Biosens. Bioelectron. 23, 1032–1038.
Zhou, H.L., Wu, T., Dong, X.L., Wang, Q., Shen, J.W., 2007. Biochem. Biophys. Res. Commun. 361, 91–96.
Zhu, Y.C., Cheng, G.J., Dong, S.J., 2002. Biophys. Chem. 97, 129–138.